



Universiteit  
Leiden  
The Netherlands

## **Efficacy, safety and novel targets in cardiovascular disease : advanced applications in APOE\*3-Leiden.CETP mice**

Pouwer, M.G.

### **Citation**

Pouwer, M. G. (2020, March 5). *Efficacy, safety and novel targets in cardiovascular disease : advanced applications in APOE\*3-Leiden.CETP mice*. Retrieved from <https://hdl.handle.net/1887/86022>

Version: Publisher's Version

License: [Licence agreement concerning inclusion of doctoral thesis in the Institutional Repository of the University of Leiden](#)

Downloaded from: <https://hdl.handle.net/1887/86022>

**Note:** To cite this publication please use the final published version (if applicable).

Cover Page



Universiteit Leiden



The handle <http://hdl.handle.net/1887/86022> holds various files of this Leiden University dissertation.

**Author:** Pouwer, M.G.

**Title:** Efficacy, safety and novel targets in cardiovascular disease : advanced applications in APOE\*3-Leiden.CETP mice

**Issue Date:** 2020-03-05

9



# Oncostatin M reduces atherosclerosis development in APOE\*3-Leiden.CETP mice and is associated with increased survival probability in humans

Danielle van Keulen, Marianne G. Pouwer, Valur Emilsson, Ljubica Perisic Matic, Elsbet J. Pieterman, Ulf Hedin, Vilmundur Gudnason, Lori L. Jennings, Kim Holmstrøm, Boye S. Nielsen, Gerard Pasterkamp, Jan H.N. Lindeman, Alain J. van Gool, Maarten D. Sollewijn Gelpke, Hans M. G. Princen\*, Dennie Tempel\*

\*These authors contributed equally

*PLoS One.* 2019 Aug 28;14(8):e0221477

## Abstract

**Objectives:** Previous studies indicate a role for Oncostatin M (OSM) in atherosclerosis and other chronic inflammatory diseases for which inhibitory antibodies are in development. However, to date no intervention studies with OSM have been performed, and its relation to coronary heart disease (CHD) has not been studied.

**Methods and Results:** Gene expression analysis on human normal arteries (n=10) and late stage/advanced carotid atherosclerotic arteries (n=127) and in situ hybridization on early human plaques (n=9) showed that OSM, and its receptors, OSM receptor (OSMR) and Leukemia Inhibitory Factor Receptor (LIFR) are expressed in normal arteries and atherosclerotic plaques. Chronic OSM administration in APOE\*3-Leiden.CETP mice (n=15/group) increased plasma E-selectin levels and monocyte adhesion to the activated endothelium independently of cholesterol but reduced the amount of inflammatory Ly-6C<sup>High</sup> monocytes and atherosclerotic lesion size and severity. Using aptamer-based proteomics profiling assays high circulating OSM levels were shown to correlate with post incident CHD survival probability in the AGES–Reykjavik study (n=5457).

**Conclusions:** Chronic OSM administration in APOE\*3-Leiden.CETP mice reduced atherosclerosis development. In line, higher serum OSM levels were correlated with improved post incident CHD survival probability in patients, suggesting a protective cardiovascular effect.

## Introduction

Cytokines have an indisputable role in all stages of atherosclerosis development. In the initial stages of the disease, cytokines induce endothelial activation leading to endothelial adhesion molecule expression and leukocyte recruitment to the activated endothelium. In later stages of the disease, cytokines are involved in smooth muscle cell (SMC) migration, foam cell formation and enhanced MMP activity leading to plaque destabilization (1,2).

Similarly, a role for Oncostatin M (OSM) in atherosclerosis has been suggested (3,4). This cytokine is secreted by activated macrophages and neutrophils and signals through the Leukemia Inhibitory Factor Receptor (LIFR) and the OSM receptor (OSMR) (5–7). OSM induces endothelial activation by increasing cytokine release, adhesion molecule expression, and leukocyte adhesion to the activated endothelium in cultured endothelial cells (8–10). Moreover, OSM reduces vascular integrity of rat blood brain barrier endothelial cells and enhances angiogenesis (11,12). Next to its effects on the endothelium, OSM enhances SMC proliferation, migration and differentiation (4,12,13).

Additional evidence for this potential role of OSM in atherosclerosis, was provided by Albasanz-Puig et al., who showed that OSM is expressed in both murine and human atherosclerotic plaques (13). Furthermore, in ApoE<sup>-/-</sup> mice, OSMR deficiency attenuated atherosclerosis development and increased plaque stability (14).

Using a different approach, we recently demonstrated that short-term OSM administration (for 3 weeks) to APOE\*3-Leiden.CETP mice increased plasma E-selectin levels, Interleukin (IL)-6 mRNA expression in the aorta and Intercellular Adhesion Molecule 1 (ICAM-1) expression and monocyte adherence to the activated endothelium in the aortic root (10). Collectively, these findings suggest that OSM may be involved in atherosclerosis development but so far this has never been studied.

The aim of this study is to investigate whether OSM is involved in atherosclerosis development in a humanized mouse model and in man. Therefore, we first investigated if OSM and its receptors are expressed in human normal and atherosclerotic arteries and if circulating OSM levels correlate with markers of endothelial activation in humans. Next, we explored the effect of long-term OSM administration on endothelial activation, atherosclerosis development and lesion composition in APOE\*3-Leiden.CETP mice, a translational model for human lipoprotein metabolism and atherosclerosis development (15). Finally, we investigated if circulating OSM levels were associated with survival probability post coronary heart disease (CHD) in humans.

## Materials and methods

### Microarray on BiKE study material

Late stage/advanced atherosclerotic plaques were obtained from patients undergoing surgery for high grade (>50%) carotid stenosis and retained within the BiKE study. Normal artery controls were obtained from nine macroscopically disease-free iliac arteries and one aorta from organ donors without history of cardiovascular disease. All samples were collected with informed consent from patients or organ donor guardians. 127 plaques from BiKE patients and 10 normal arteries were analyzed by Affymetrix HGU133 plus 2.0 GeneChip microarrays. Robust multiarray average normalization was performed and processed gene expression data was transformed in log<sup>2</sup>-scale. The microarray dataset is available from Gene Expression Omnibus (GSE21545). The BiKE study cohort demographics, details of sample collection, processing, and analyses were previously described (16).

### In situ hybridization (ISH) on SOCRATES study material

Early stage atherosclerotic lesions for in situ hybridization were obtained from the SOCRATES biobank (Leiden University Medical Center, the Netherlands). Details of this biobank have been described previously (17). Briefly, this biobank contains aortic wall patches obtained during kidney transplantation with grafts derived from cadaveric donors. Sample collection and handling were performed in accordance with the guidelines of the Medical and Ethical Committee in Leiden, the Netherlands, and the code of conduct of the Dutch Federation of Biomedical Scientific Societies (<https://www.federa.org/?s=1&m=82&p=0&v=4#827>). Chromogenic mRNA-ISH was essentially performed as previously described (18,19) on 9 atherosclerotic lesions from the SOCRATES biobank. For detection of the OSM, OSMR and LIFR mRNAs, ISH was performed in a Ventana Discovery ULTRA instrument (Ventana Medical Systems Inc., AZ, USA) using the ACD RNAscope® 2.5 Red Kit (Advanced Cell Diagnostics, Newark, CA, USA) and the mRNA Discovery ULTRA RED 4.0 procedure. RNAscope® 2.5 VS. Probes for Hs-OSM (#456389), Hs-OSMR-tv1 (#445699) and Hs-LIFR (#441029) were designed by the probe manufacturer (Advanced Cell Diagnostics). FFPE sections (5 µm) were applied to Superfrost Plus (Thermo Fisher Scientific) slides, and all operations including deparaffinization, pretreatment, ISH and counterstaining using hematoxylin were performed in a Ventana Discovery ULTRA instrument. Following the ISH-procedure in the Ventana instrument, slides were washed in lukewarm tap water with detergent until oil from the slides was fully removed. Subsequently, slides were washed in demineralized water, air dried and mounted in EcoMount mounting medium (Advanced Cell Diagnostics) prior to scanning in a bright-field whole-slide scanner (Axio Scan.Z1, Zeiss, Oberkochen Germany) using a 20x objective. The resulting digital images were inspected and regions of interest were selected.

## Proteomics on AGES-Reykjavik study material

Association between OSM levels and IL-6, vascular cell adhesion molecule (VCAM)-1, P-selectin, E-selectin, ICAM-1 and Monocyte chemoattractant protein-1 (MCP-1) levels, and between OSM levels and survival were explored in the AGES-Reykjavik cohort (n=5457) (20), a single-center prospective population-based study of deeply phenotyped elderly European Caucasians (aged 66 through 96, mean age 75±6 years) who survived the 50-year-long prospective Reykjavik study. Phenotype description, patient numbers and other details related to the present study have been described previously (21). The AGES-Reykjavik study was approved by the NBC in Iceland (approval number VSN-00-063), the National Institute on Aging Intramural Institutional Review Board (USA), and the Data Protection Authority in Iceland. We applied a custom version of the Slow Off-rate Modified Aptamer (SOMAmer) platform targeting proteins known or predicted to be found in the extracellular milieu, including the predicted extracellular domains of single- and certain multi-pass transmembrane proteins, as previously described (21).

For survival analysis post CHD, we used 698 incident CHD cases exhibiting 307 deaths during the survival follow-up period of 12 years. Follow-up time for survival post incident CHD was defined as the time from 28 days after an incident CHD event until death from any cause or end of follow-up time.

## Animals and treatments

Sixty-five female in-house bred APOE\*3-Leiden.CETP transgenic mice (10-15 weeks of age) were used. Mice were housed under standard conditions with a 12h light-dark cycle and free access to food and water. Body weight, food intake and clinical signs of behavior were monitored regularly. Mice received a Western type diet (semi-synthetic containing 15 w/w% cacao butter and 0.15% dietary cholesterol, Altromin, Tiel, the Netherlands). At t=0 weeks, after a run-in period of 3 weeks, mice were matched based on body weight, age, plasma total cholesterol and E-selectin levels in 4 groups: a control group, and three intervention groups, two of which were treated with 10 or 30 µg/kg/day OSM for 16 weeks, and an initial priming group, which received 30 µg/kg/day OSM for the first 5.5 weeks only. All groups consisted of 15 mice except for the control group which had an additional 5 mice to monitor the atherosclerosis development. Five mice were removed from the study based on human end-point criteria and were excluded from all analyses: 2 mice in the 16 week 30 µg/kg/day OSM group and 1 in each of the other 3 groups. At t=0 weeks, an ALZET® Osmotic Pump Type 1004 (Durect, Cupertino, CA) containing either 10 or 30 µg/kg/day murine OSM (R&D systems, Minneapolis, MN) or the vehicle (PBS + 1% mouse serum) was placed subcutaneously in the flank and were replaced at t=5.5 and 11 weeks. Doses were based on our previous research (10). Prior to surgery, mice received the analgesic Carprofen (5 mg/kg s.c.) and were anesthetized with isoflurane (induction 4%, maintenance 2%). EDTA blood samples were drawn after a 4 hour fast at t=0, 4, 8, 12 and 16 weeks for determination of total cholesterol and inflammatory markers. At t=12 weeks,



4 mice from the control group were euthanized to assess atherosclerosis development for the determination of the end-point of the study. At t=16 weeks, mice were euthanized by gradual CO<sub>2</sub> inhalation. Death was confirmed by exsanguination (via heart puncture) and hearts were isolated. All animal experiments were performed conform the guidelines from Directive 2010/63/EU of the European Parliament on the protection of animals used for scientific purposes or the NIH guidelines. Approval was granted by the ethics committee on animal experiments (approval reference number DEC-3683) and the institutional animal welfare body (approval reference number TNO-255).

### **Plasma parameters**

Plasma cholesterol was measured spectrophotometrically with enzymatic assays (Roche Diagnostics). E-selectin and MCP-1 were measured with ELISA kits from R&D (Minneapolis, MA, USA), and Serum Amyloid A (SAA) with an ELISA kit from Tridelata Development Limited (Maynooth, County Kildare, Ireland). All assays were performed according to the manufacturer's instructions.

### **Histological assessment of atherosclerosis and plaque composition**

Atherosclerotic lesion area and severity were assessed in the aortic root area, as reported previously (22,23). Briefly, the aortic root was identified by the appearance of aortic valve leaflets, and serial cross-sections of the entire aortic root area (5 µm thick with intervals of 50 µm) were mounted on 3-aminopropyl triethoxysilane-coated slides and stained with haematoxylin-phloxine-saffron (HPS). For each mouse, the lesion area was measured in 4 subsequent sections. Each section consisted of 3 segments (separated by the valves). For determination of atherosclerotic lesion severity, the lesions were classified into five categories according to the American Heart Association (AHA) criteria (24): type 1 (early fatty streak), type 2 (regular fatty streak), type 3 (mild plaque), type 4 (moderate plaque), and type 5 (severe plaque). The total lesion area was calculated per cross-section. Due to a technical error one mouse of the OSM (30 µg/kg, 16 weeks) was excluded from analysis. Lesion severity was calculated as relative amount of type I-V lesions in which the lesion-free segments are included. From this, the relative amounts of lesion-free segments and diseased segments were calculated, and the relative amount of diseased segments was further subdivided into type I-V lesions, where types I-III refer to mild, and types IV-V to severe lesions. Lesion composition of type IV and V lesions was assessed after double immunostaining with anti-α smooth muscle actin (1:400; PROGEN Biotechnik GmbH, Germany) for smooth muscle cells (SMC), and anti-mouse MAC-3 (1:400; BD Pharmingen, the Netherlands) for macrophages. Anti-α smooth muscle actin was labeled with Vina green (Biocare Medical, Pacheco, USA), and MAC-3 with DAB (Vector laboratories, Burlingame, USA). After slides were scanned and analyzed, cover slips were detached overnight in xylene and Sirius Red staining for collagen was performed. The necrotic area was measured in the Sirius Red-stained slides. Lesion stability index, as the ratio of collagen

and  $\alpha$ SMC area (i.e. stabilization factors) to macrophage and necrotic area (i.e. destabilization factors) was calculated as described previously (22). Lesion composition was assessed in all type IV-V lesions with a mean of  $5.9 \pm 3.1$  lesions in control,  $5.6 \pm 2.5$  lesions in OSM  $10 \mu\text{g}/\text{kg}/\text{d}$ ,  $2.9 \pm 2.0$  lesions in OSM  $30 \mu\text{g}/\text{kg}/\text{d}$  temporary and  $2.8 \pm 2.9$  lesions in OSM  $30 \mu\text{g}/\text{kg}/\text{d}$ . Eight mice were excluded from analysis as there were no type IV-V lesions present ( $n=1$  in control;  $n=4$  in OSM  $30 \mu\text{g}/\text{kg}/\text{d}$  temporary and  $n=3$  in OSM  $30 \mu\text{g}/\text{kg}/\text{d}$ ). In each segment used for lesion quantification, ICAM-1 expression and the number of monocytes adhering to the endothelium were counted after immunostaining with mouse monoclonal ICAM-1 antibody (1:400; Santa Cruz Biotechnology, Dallas, USA) and AIA 31240 antibody (1:500; Accurate Chemical and Scientific, New York, USA) respectively (25). NLRP3 expression in the macrophages was quantified after staining with rabbit polyclonal antibody to NLRP3 (1:400; Abcam, Cambridge, UK). All slides were scanned by an Aperio AT2 slide scanner (Leica Biosystems). Atherosclerotic area, monocyte adherence and ICAM-1 expression were measured in Image Scope (version 12-12-2015), and the area that stained positive for  $\alpha$ SMA, MAC-3, Sirius Red and NLRP3 in the plaques was quantified automatically in Fiji (version 30-5-2017) using a threshold method.

### Flow cytometry

To analyze the different monocyte subsets,  $25 \mu\text{L}$  whole blood was incubated with antibodies against CD11b (APC-eFluor780-conjugated, eBioscience, San Diego, California, USA), Ly-6C (eFluor450-conjugated, eBioscience, San Diego, California, USA) and Ly-6G (A647-conjugated, Biolegend, San Diego, California, USA) for 30 min at RT. Erythrocytes were lysed with lysis buffer (deionized water with 168 mM ammonium chloride (Merck, Darmstadt, Germany), 9.99 mM potassium bicarbonate (Merck, Darmstadt, Germany) and 0.11 mM  $\text{Na}_2\text{EDTA}$  (Sigma-Aldrich, St. Louis, MO, USA)) for 10 min on ice and remaining erythrocytes were lysed with fresh lysis buffer for 5 min on ice. After washing, cells were fixed in 1% paraformaldehyde for 10 min on ice, measured with flow cytometry (Gallios, Beckman Coulter Fullerton, CA, USA) and analyzed with Kaluza Flow Analysis Software Version 2.1 (Beckman Coulter). Monocytes were defined as CD11b+Ly-6G-.

### Statistics

BiKE transcriptomic dataset analyses were performed with GraphPad Prism 6 and Bioconductor software using a linear regression model adjusted for age and gender and a two-sided Student's t-test assuming non-equal deviation, with correction for multiple comparisons according to Bonferroni, as previously described (16). Data are presented as mean  $\pm$  SD and adjusted  $p < 0.05$  was considered to indicate statistical significance.

Prior to protein data analyses, we applied a Box-Cox transformation on the proteins to improve normality, symmetry and to maintain all protein variables on a similar scale (21). For protein to protein correlation we used linear regression analysis. Given consistency in terms of sample handling including time from blood draw to processing, same personnel

handling all specimens and the ethnic homogeneity of the Icelandic population we adjusted only for age and sex in all our regression analyses.

Mouse data analyses were performed with GraphPad Prism 7.04 and IBM SPSS v25.0. Data are presented as mean  $\pm$  SD. Normally (Gaussian) distributed mouse parameters were analyzed with a t-test or one-way ANOVA and not normally distributed mouse parameters with a Kruskal-Wallis test followed by a Mann-Whitney U test if significant. A significant difference between the 16 week 10 and 16 week 30  $\mu\text{g}/\text{kg}/\text{day}$  groups was considered as a dose-dependent difference. The rejection criteria were adjusted using a Bonferroni-Holm correction. Correlation between plaque size and Ly-6C<sup>High</sup> monocytes was tested with a Pearson correlation. A two-tailed p-value of 0.05 was regarded statistically significant in all analyses.

Cox proportional hazards regression was used for post incident CHD and Kaplan-Meier plots were applied to display survival data.

## Results

### **mRNAs coding for OSM, OSMR and LIFR are present in human atherosclerotic plaques**

To explore if OSM signaling can be involved in human plaque development, we first investigated if OSM mRNA and the mRNAs for the receptors for OSM, OSMR and LIFR, were present in late-stage human carotid plaques from the BiKE study. Gene expression analysis revealed presence of OSMR, LIFR and OSM mRNAs at low to moderate levels. mRNA expression of both receptors was significantly downregulated in plaques ( $p < 0.0001$ ) compared to normal arteries, while OSM expression was significantly increased ( $p = 0.003$ ) (**Figure 1A-C**). OSM mRNA expression positively correlated with macrophage markers and negatively with SMC markers (**Table 1**). Subsequent in situ hybridization confirmed the presence of OSMR, LIFR and OSM mRNAs in all investigated atherosclerotic plaque stages (**Figure 1D-O**), which is reflected in **Table 2**.

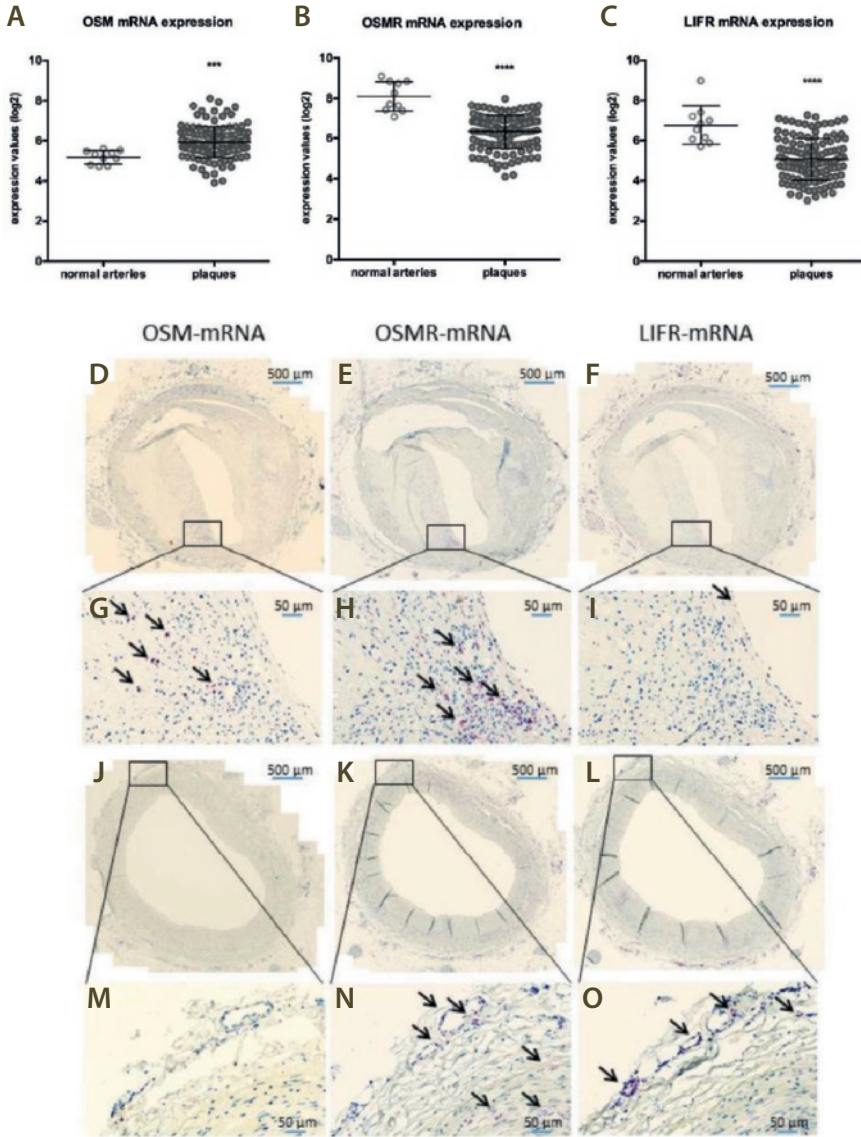


**Figure 1** OSM, OSMR and LIFR mRNA expression is present in human atherosclerotic plaques. mRNA expression was measured in normal arteries and in carotid plaques by microarray analysis (A-C) and ISH was used to visualize OSM, OSMR and LIFR mRNA expression (red spots and shown by the black arrows) in two different stages of atherosclerosis development, the late fibroatheroma (D-I) and intimal xanthoma (J-O). \*\*\* $p < 0.001$ , \*\*\*\* $p < 0.0001$ . Abbreviations: ISH, in situ hybridization.

**Table 1** Correlation between OSM and genes of interest in plaques

	Gene symbol	Pearson r	p-value	Significance level
<b>Cell type markers</b>				
<i>Smooth muscle cells</i>				
Myosin heavy chain 11	MYH11	-0.4327	< 0.0001	****
Smoothelin	SMTN	-0.4437	< 0.0001	****
Alpha smooth muscle actin	ACTA2	-0.3476	< 0.0001	****
Myocardin	MYOCD	-0.4119	< 0.0001	****
Transgelin	TAGLN	-0.3127	0.0004	***
<i>Endothelial cells</i>				
von Willebrand factor	VWF	0.1486	0.0967	ns
Pecam-1 (CD31)	PECAM1	0.3009	0.0006	***
<i>Dendritic cells</i>				
Itgax (CD11c)	ITGAX	0.4738	< 0.0001	****
Ly75 (CD205)	LY75	-0.03098	0.7295	ns
CD80	CD80	0.6013	< 0.0001	****
<i>T Lymphocytes</i>				
CD11b	ITGAM	0.4048	< 0.0001	****
ITGAL	ITGAL	0.5012	< 0.0001	****
CD27	CD27	0.107	0.233	ns
CD28	CD28	0.2859	0.0012	**
CD3 delta	CD3D	0.3678	< 0.0001	****
CD4	CD4	0.1078	0.2295	ns
CD8A	CD8A	0.2258	0.0107	*
PTPRC (CD45RA)	PTPRC	0.3758	< 0.0001	****
CD69	CD69	0.4909	< 0.0001	****
ITGAE	ITGAE	0.2827	0.0013	**
FABP4	FABP4	0.3884	< 0.0001	****
<i>Macrophages</i>				
CD83	CD83	0.5474	< 0.0001	****
CD86	CD86	0.4934	< 0.0001	****
CD163	CD163	0.4434	< 0.0001	****
TNFRSF9	TNFRSF9	0.3696	< 0.0001	****
CD40	CD40	0.3422	< 0.0001	****
CD36	CD36	0.4466	< 0.0001	****
<b>Inflammation/ Apoptosis Calcification markers</b>				
IL-1beta	IL1B	0.5657	< 0.0001	****
NFKB	NFKB1	0.1764	0.0481	*

**Table 1** Continued

	Gene symbol	Pearson r	p-value	Significance level
<b>Inflammation/ Apoptosis Calcification markers</b>				
MCP-1	CCL2	0.5311	< 0.0001	****
Caspase-3	CASP3	0.2726	0.002	**
Caspase-7	CASP7	0.05738	0.5233	ns
Caspase-9	CASP9	0.2318	0.009	**
BCL2	BCL2	0.2761	0.0018	**
RANTES	CCL5	0.3821	< 0.0001	****
BMP4	BMP4	-0.1434	0.1091	ns
<b>Extracellular matrix/ degradation</b>				
MMP9	MMP9	0.4202	< 0.0001	****
TIMP1	TIMP1	0.3891	< 0.0001	****
<b>Growth factors</b>				
TGFB1	TGFB1	0.4113	< 0.0001	****
TGFA	TGFA	0.328	0.0002	***
IGF1	IGF1	0.256	0.0038	**
PDGFA	PDGFA	-0.02346	0.7943	ns
PDGFB	PDGFB	0.2417	0.0064	**
PDGFC	PDGFC	-0.2382	0.0072	**
PDGFD	PDGFD	-0.2889	0.001	**
<b>Chemokines and receptors</b>				
Interferon gamma	IFNG	0.2032	0.0225	*
IL2	IL2	0.2446	0.0058	**
IL4	IL4	0.03414	0.7043	ns
IL5	IL5	0.1947	0.0289	*
IL6	IL6	0.5659	< 0.0001	****
IL9	IL9	0.05453	0.5442	ns
IL10	IL10	0.4213	< 0.0001	****

Pearson correlation analyses were calculated from n=127 human plaque microarrays, p-values are corrected for multiple comparisons according to the Bonferroni method. Correlation considered weak if  $r < 0.3$  moderate if  $0.3 < r < 0.5$  and strong if  $r > 0.5$ . \* $p < 0.05$ , \*\* $p < 0.01$ , \*\*\* $p < 0.001$ , \*\*\*\* $p < 0.0001$

**Table 2** Quantification of ISH signal in various atherosclerotic plaque stages

		mRNA expression		
		OSM	OSMR	LIFR
<b>Adaptive Intimal Thickening</b>	<b>Neo-intima</b>	1	2	2
	<b>Media</b>	1	3	2
	<b>Adventitia</b>	1	3	3
<b>Intimal Xanthoma</b>	<b>Neo-intima</b>	1	2	2
	<b>Media</b>	0	2	3
	<b>Adventitia</b>	0	2	3
<b>Pathological Intimal Thickening</b>	<b>Neo-intima</b>	1	2	2
	<b>Media</b>	1	3	2
	<b>Adventitia</b>	1	3	3
<b>Early Fibroatheroma</b>	<b>Neo-intima</b>	2	2	2
	<b>Media</b>	1	2	2
	<b>Adventitia</b>	1	3	3
<b>Late Fibroatheroma</b>	<b>Neo-intima</b>	2	2	2
	<b>Media</b>	2	2	2
	<b>Adventitia</b>	1	2	4
<b>Fibrous Calcified Plaque</b>	<b>Neo-intima</b>	2	2	2
	<b>Media</b>	1	3	2
	<b>Adventitia</b>	1	3	2

The amount of ISH signal was scored in various atherosclerotic plaque stages. A general score and a single cell score was given. 0 = no signal, 1 = few cells expressing mRNA, 2 = low expression, 3 = moderate expression and 4 = high expression. Abbreviations: ISH, in situ hybridization.

### **OSM is associated with endothelial activation markers IL-6 and VCAM-1 in humans**

We previously found that OSM induces endothelial activation both in vitro in human endothelial cells and in vivo in APOE\*3-Leiden.CETP mice (10). To investigate if OSM can be linked with markers of endothelial activation in a human setting as well, we measured serum levels of OSM and several circulating endothelial activation markers in the AGES-Reykjavik study. OSM levels modestly correlated with IL-6 ( $\beta = 0.210$ ,  $p=5*10^{-56}$ ) and VCAM-1 ( $\beta = 0.130$ ,  $p=4*10^{-20}$ ) levels, but inversely with P-Selectin ( $\beta = -0.115$ ,  $p=5*10^{-17}$ ), E-Selectin ( $\beta = -0.092$ ,  $p=2*10^{-11}$ ) and ICAM-1 ( $\beta = -0.013$ ,  $p=5*10^{-7}$ ) levels (**Figure 2**). No correlation of OSM with MCP-1 was observed.

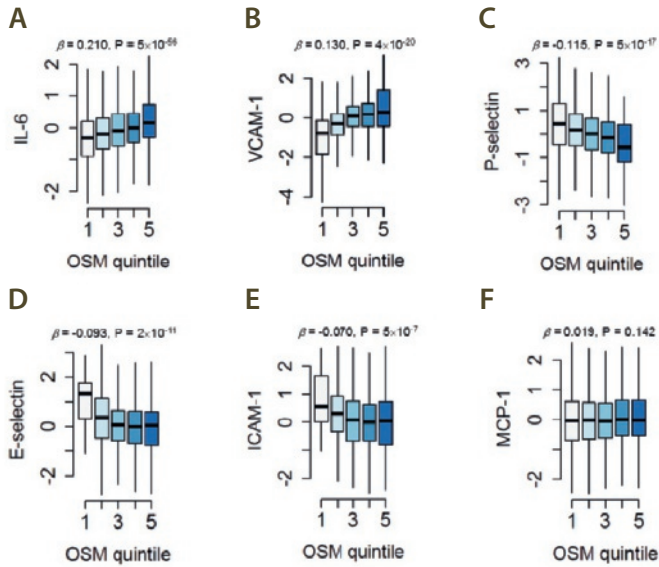


**Figure 2** OSM is associated with endothelial activation markers. Association of serum IL-6 (A), VCAM-1 (B), P-selectin (C), E-selectin (D), ICAM-1 (E) and MCP-1 (F) levels (y-axis) with quintiles of increasing OSM serum levels (x-axis) using specific aptamers measured in 5457 subjects of the AGES cohort. Linear regression analyses were used to test for association.

### Chronic exposure to OSM results in a pro-inflammatory vascular phenotype in APOE\*3-Leiden.CETP mice

The above and our previous data (10) suggest a role for OSM in atherosclerosis development. Therefore, we performed a long-term study in which we administered OSM to APOE\*3-Leiden.CETP mice for 16 weeks. To specifically investigate the effect of OSM on the initiation of atherosclerosis, we added an initial priming group that was treated with OSM only for the first 5.5 weeks of the study. As previous studies had a much shorter duration (ranging from 6 hours to 3 weeks), we first investigated if long-term OSM treatment persistently causes an inflammatory phenotype by measuring E-selectin, MCP-1 and SAA plasma levels, as markers of vessel wall, general and liver-derived inflammation. Treatment groups receiving either 10  $\mu\text{g}/\text{kg}/\text{day}$  ( $p=0.002$ ) or 30  $\mu\text{g}/\text{kg}/\text{day}$  ( $p<0.001$ ) OSM for 16 weeks showed markedly increased E-selectin levels at all time points and a dose-dependent increase at  $t=4$  ( $p<0.01$ ) and 8 weeks ( $p<0.01$ ). The group receiving 5.5 weeks 30  $\mu\text{g}/\text{kg}/\text{day}$  OSM treatment also showed markedly increased E-selectin levels at  $t=4$  ( $p<0.001$ ), though after discontinuation of OSM treatment, E-selectin levels dropped and declined to similar levels as the control group. MCP-1 and SAA levels did not differ between the OSM treated groups and control (**Figure 3A-C**). Also, no statistical difference



was observed in ICAM-1 expression at the endothelium in the aortic root area (**Figure 3D**). In contrast, monocyte adhesion, as functional marker of endothelial activation, in the aortic root area was increased from  $4.9 \pm 3.3$  monocytes per cross-section in the control group to  $17.9 \pm 10.7$  in the 16 weeks 30  $\mu\text{g}/\text{kg}/\text{day}$  group ( $p=0.003$ ) (**Figure 3E**). These results indicate that continuous OSM exposure results in a sustained pro-inflammatory vascular phenotype, even after 16 weeks of treatment.

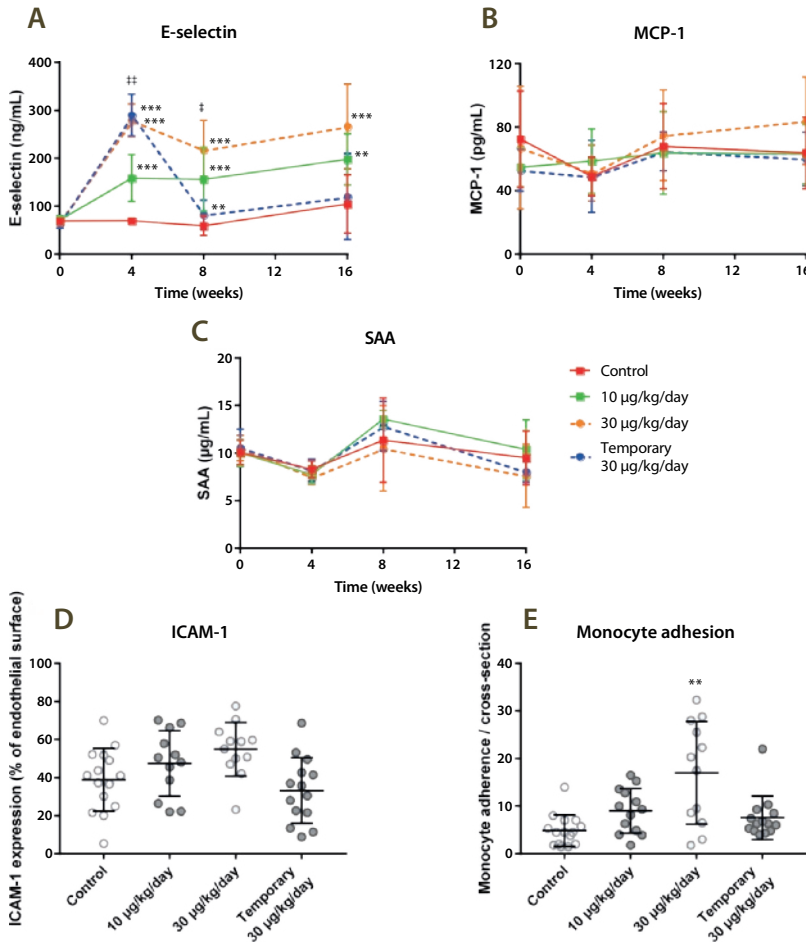


**Figure 3** OSM induces a pro-inflammatory vascular phenotype in APOE\*3-Leiden.CETP mice. Plasma E-selectin, MCP-1 and SAA (A-C) were measured at multiple time points during the study. Monocyte adhesion (D) and endothelial ICAM-1 expression were assessed per cross-section in the aortic root area (E). Data represent mean  $\pm$  SD ( $n=12-20$ ).  $\ddagger p<0.05$  compared to 10  $\mu\text{g}/\text{kg}/\text{day}$ ;  $**p<0.01$  compared to control;  $\ddagger\ddagger p<0.01$  compared to 10  $\mu\text{g}/\text{kg}/\text{day}$ ;  $***p<0.001$  compared to control.

### OSM reduces atherosclerotic lesion area and severity in APOE\*3-Leiden.CETP mice

Total plasma cholesterol levels, a risk factor for cardiovascular disease, did not differ between any of the groups (data not shown). Atherosclerotic lesion size and severity were investigated in the aortic root area of which representative pictures are shown in **Figure 4**. The control group had an average lesion size of  $119 \pm 64 *1000 \mu\text{m}^2$ . In the 5.5 week 30  $\mu\text{g}/\text{kg}/\text{day}$  OSM group, plaque size was reduced by 59% ( $p=0.002$ ) and in the 16 week 30  $\mu\text{g}/\text{kg}/\text{day}$  OSM group by 58% ( $p=0.002$ ), while the 16 week 10  $\mu\text{g}/\text{kg}/\text{day}$  OSM treated group did not differ from the control (**Figure 5A**). The decrease in plaque area was dose-dependent ( $p=0.006$ ). In the control group,  $62 \pm 27\%$  of the lesions were classified as severe lesions, while only  $23 \pm 22\%$  ( $p=0.001$ ) and  $26 \pm 24\%$  ( $p=0.002$ ) of the lesions were severe in the 16 week 30  $\mu\text{g}/\text{kg}/\text{day}$  and 5.5 week 30  $\mu\text{g}/\text{kg}/\text{day}$  OSM treated group,

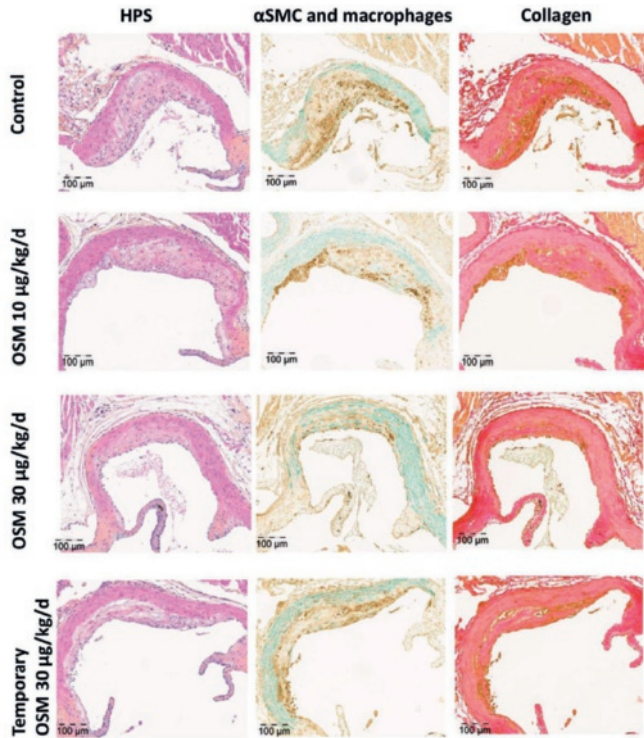


**Figure 4** Effect of OSM on plaque composition in APOE\*3-Leiden.CETP mice. Representative pictures showing severe lesion types (type IV and V) stained with HPS staining, SMC staining (green), macrophage staining (brown) and collagen staining (red) to determine the effect of OSM on the lesion composition.

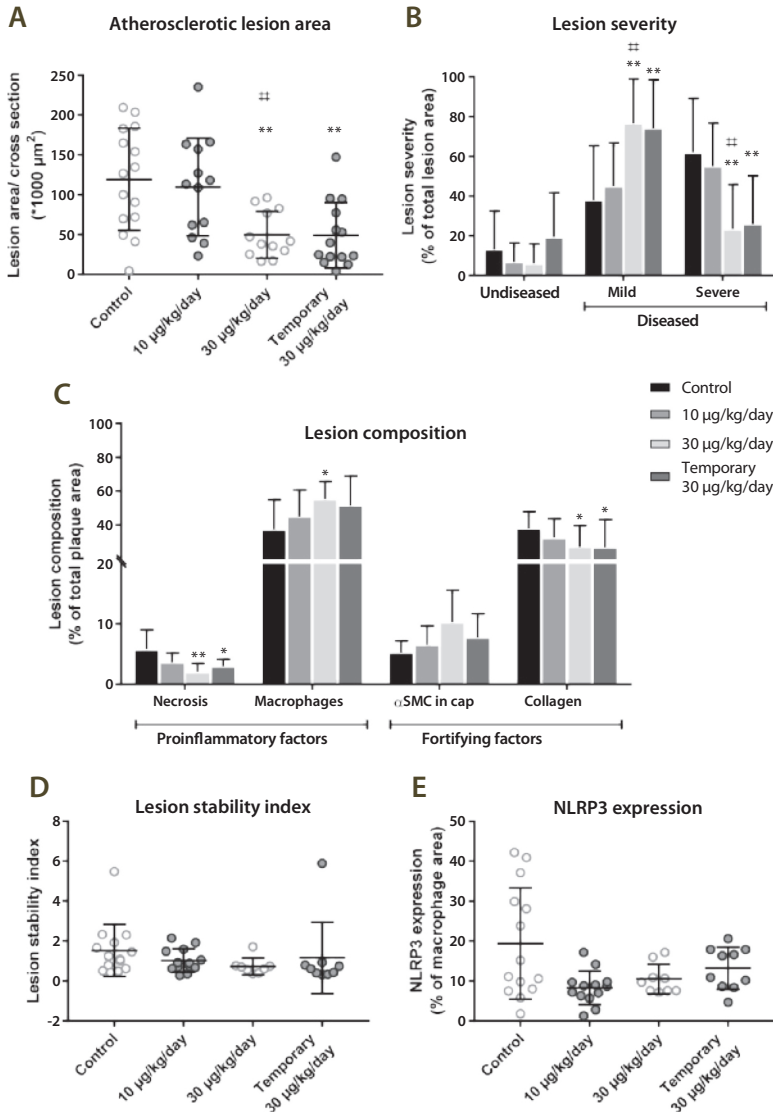


**Figure 5** OSM reduces lesion size and severity in APOE\*3-Leiden.CETP mice. The atherosclerotic lesion size was determined in the aortic root area (A) and the lesions were classified as mild (type I-III) or severe (IV and V) lesions (B). Furthermore, the amount of necrosis, macrophages, smooth muscle cells and collagen was quantified (C) and the lesion stability index was calculated by dividing the summed proportions of SMCs and collagen, as stabilizing factors, by the summed proportions of necrosis and macrophages, as destabilizing factors (D). Additionally, the amount of NLRP3 expression was examined as percentage of the macrophage area (E). Data represent mean  $\pm$  SD (n=9-15). \*p<0.05 \*\*p<0.01 compared to control; †† p<0.01 compared to 10  $\mu\text{g}/\text{kg}/\text{day}$ .

respectively. Again, the 16 week 10  $\mu\text{g}/\text{kg}/\text{day}$  OSM treatment group did not differ from the control group. In line with plaque area, we observed a dose-dependent decrease in lesion severity ( $p=0.003$ ) (**Figure 5B**). Collectively, these results show that early continuous exposure to OSM reduces atherosclerotic lesion size and severity independently from plasma cholesterol in APOE\*3-Leiden.CETP mice.

### **OSM has no effect on the stability of severe lesions in APOE\*3-Leiden.CETP mice**

To assess the effect of OSM treatment on plaque stability of the severe lesions, we determined the amount of necrosis and macrophages, as indicators of unstable plaques and the amount of SMCs and collagen, as indicators of stable plaques (**Figure 5C**) in the severe lesions. Lesions in the control group consisted of  $6 \pm 3\%$  necrosis,  $37 \pm 18\%$  macrophages,  $5 \pm 2\%$  SMCs and  $38 \pm 10\%$  collagen. The amount of necrosis was decreased to  $3 \pm 1\%$  in the 5.5 week 30  $\mu\text{g}/\text{kg}/\text{day}$  OSM group ( $p=0.012$ ) and to  $2 \pm 1\%$  in the 16 week 30  $\mu\text{g}/\text{kg}/\text{day}$  OSM group ( $p=0.01$ ), while the macrophage content was slightly increased in the 16 week 30  $\mu\text{g}/\text{kg}/\text{day}$  OSM group ( $55 \pm 10\%$ ) ( $p=0.016$ ) only. The collagen content was decreased in the 5.5 week 30  $\mu\text{g}/\text{kg}/\text{day}$  OSM group to  $28 \pm 17\%$  ( $p=0.012$ ) and to  $27 \pm 13\%$  in the 16 week 30  $\mu\text{g}/\text{kg}/\text{day}$  OSM group ( $p=0.018$ ). No difference was observed in SMC content. The plaque composition of the 16 week 10  $\mu\text{g}/\text{kg}/\text{day}$  OSM group was similar as in the control group. No differences were observed in the plaque stability ratio between the control and OSM treated groups (**Figure 5D**). As the amount of macrophages is not necessarily a measure for macrophage activity, we measured the expression of the caspase-1-activating inflammasome protein NLRP3 as marker of macrophage activation (26). No significant difference was observed in NLRP3 expression in the plaque area (**Figure 5E**). In conclusion, although OSM does affect lesion composition by slightly increasing the amount of macrophages and decreasing the amount of necrosis and collagen, it does not affect overall plaque stability of the severe lesions.

### **OSM reduces the inflammatory Ly-6C<sup>High</sup> monocyte subset**

No difference in the percentage of circulating CD11b+ cells was observed between the groups (**Figure 6A**). As the Ly-6C<sup>High</sup> monocyte subset is linked to atherosclerosis development (27), we investigated the effect of OSM on the circulating monocyte subtype composition (**Figure 7**). In the control group  $20.8 \pm 6.5\%$  of the monocytes belonged to the Ly-6C<sup>High</sup> subset and  $79.2 \pm 6.5\%$  to the Ly-6C<sup>Low+Intermediate</sup> subset. The amount of Ly-6C<sup>High</sup> monocytes was decreased to  $13.2 \pm 3.8\%$  in the 16 week 30  $\mu\text{g}/\text{kg}/\text{day}$  OSM group ( $p=0.004$ ) and the amount of Ly-6C<sup>Low+Intermediate</sup> monocytes increased to  $86.8 \pm 3.8\%$  ( $p=0.004$ ) (**Figure 6B and C**). The Ly-6C<sup>High</sup> subset showed a positive correlation with lesion size ( $r=0.303$ ,  $p=0.029$ ), supporting a role of the Ly-6C<sup>High</sup> monocytes in the development of atherosclerosis (**Figure 6D**). Thus, OSM decreases the percentage of Ly-6C<sup>High</sup> monocytes which may contribute to the smaller atherosclerotic lesion size.

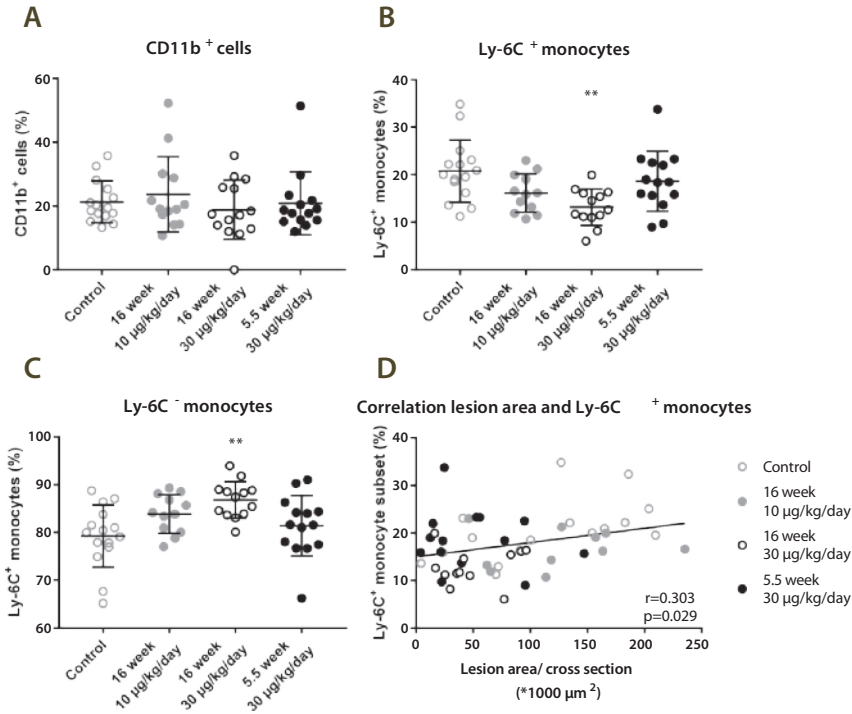


**Figure 6** OSM reduces the percentage of circulating Ly-6C<sup>High</sup> monocytes. No difference in percentage of CD11b<sup>+</sup> cells was observed between the groups (A). But, APOE\*3-Leiden.CETP mice treated with OSM have a higher percentage of circulating Ly-6C<sup>High</sup> monocytes (B) and a lower percentage of circulating Ly-6C<sup>Low+Intermediate</sup> monocytes (C). The percentage of Ly-6C<sup>High</sup> monocytes was correlated with an increased lesion size (D). Data represent mean  $\pm$  SD (n=12-20). \*\*p<0.01 compared to control.

### Serum OSM levels are associated with increased post incident CHD in humans

We next explored if variable levels of OSM in the human circulation were associated with survival probability in the AGES-Reykjavik study. We found that higher serum OSM levels were associated with increased survival probability post incident CHD (HR=0.838,  $p=2*10^{-6}$ ) (Figure 8A), also using adjusted survival curves for the Cox model (28) (Figure 8B). Thus, elevated levels of OSM predicted reduced mortality in humans.

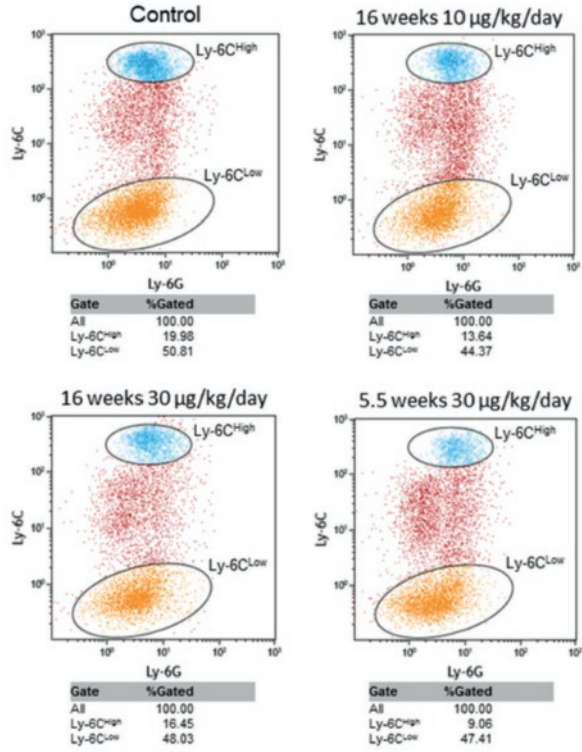


**Figure 7** Representative pictures of the distribution of the Ly-6C monocyte subsets. Based on the Ly-6C expression, monocytes were distributed into 3 monocyte subsets, the Ly-6C<sup>Low</sup>, Ly-6C<sup>Intermediate</sup> and Ly-6C<sup>High</sup> monocyte subset.

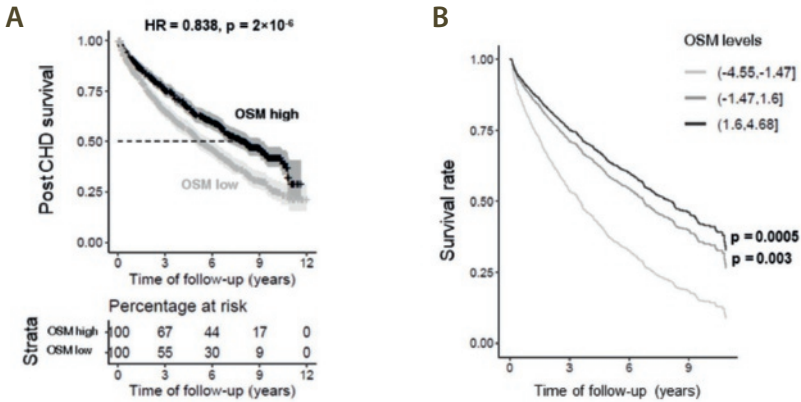


**Figure 8** High OSM is associated with reduced post CHD mortality. Serum OSM levels of CHD patients were significantly associated with CHD related mortality rates when comparing the lower 25% quantile to the upper 75% quantile in OSM levels (hazard ratio (HR)=0.838,  $p=2 \times 10^{-6}$ ) (A), and in the adjusted survival curves for the Cox model for three groups of OSM protein levels (top vs. bottom HR=0.618,  $p=0.0005$ ) (B).

## Discussion

In the present study, we showed that mRNAs coding for OSM as well as its receptors, OSMR and LIFR, were expressed in human normal arteries and carotid atherosclerotic plaques. We demonstrated that serum OSM levels in humans were positively correlated with several but not with other well-known markers of endothelial activation. Chronic OSM administration to APOE\*3-Leiden.CETP mice reduced atherosclerotic lesion size and severity even after initial priming. In line with these data, increased OSM levels in humans were associated with decreased post incident CHD mortality.

Extending the previous finding by Albasanz-Puig et al (13), who showed that OSM is present in both human and murine atherosclerotic plaques, we here demonstrated the presence of OSMR and LIFR mRNA in human normal and atherosclerotic arteries as well. The relatively higher OSMR and LIFR expression in normal arteries compared to atherosclerotic arteries may be explained by the high expression of the receptors on endothelial and vascular SMCs (8,29). These cells make up a relatively large proportion of the normal artery, but less of the atherosclerotic plaque, in which there is influx and proliferation of inflammatory cells, which might dilute OSMR and LIFR expression. The opposite can be reasoned for the increased OSM expression in atherosclerotic arteries, as OSM is mainly produced by activated macrophages and neutrophils (5,6,30). Moreover, OSMR and LIFR expression may be downregulated in endothelial and SMCs in plaques compared to

endothelial and SMCs in normal arteries. Besides, the chronic inflammatory state during atherosclerosis development drives vascular SMC differentiation, which reduces the expression of SMC specific markers (31) and may therefore also reduce expression of LIFR and OSMR. This contention is in line with our observation that OSM is negatively correlated with SMC markers and with Kakutani et al., who showed that OSM induces SMC differentiation (4).

The correlation of OSM with IL-6 and VCAM-1 in the AGES-Reykjavik study is in line with previous findings *in vitro* (10). However, the inverse association of OSM with E-selectin and ICAM-1 contradicts with previous data showing increased levels induced by OSM in human endothelial cells *in vitro* (10) and increased serum E-selectin levels in APOE\*3-Leiden.CETP mice. The absence of a positive correlation between OSM and ICAM-1, E-selectin and P-selectin may be caused by statin use in the AGES-Reykjavik study (approx. 22%) (21), as statins reduce ICAM-1, E-selectin and P-selectin plasma levels in patients with coronary artery disease (32). Regardless, mice treated with OSM in the present study did show increased serum E-selectin levels which dropped after discontinuation of OSM treatment, indicating a causal relationship between OSM and E-selectin *in vivo* in mice.

As our present study had a much longer duration than previous intervention studies with OSM in mice (9,10), we first verified if the previously observed short-term inflammatory state (10) is also present after 16 weeks of OSM administration. OSM increased plasma E-selectin levels and monocyte adhesion in the aortic root area, similarly as in our previous study (10), indicating that OSM induces a sustained inflammatory state even after long-term OSM treatment. Although inflammation has been reported to contribute to atherosclerosis development (33), our results show, to our knowledge for the first time, that long-term chronic OSM treatment independently of cholesterol-lowering, results in significantly smaller and less severe atherosclerotic lesions in APOE\*3-Leiden.CETP mice, clearly indicating that prolonged exposure to OSM has anti-atherogenic effects. Previously, Zhang et al., using a different approach, showed that OSMR deficient ApoE<sup>-/-</sup> mice have smaller and more stable plaques than their OSMR expressing littermates (14), suggesting that signaling via the LIFR alone or prevention of IL-31 and OSM signaling through OSMR (34) has a similar beneficial effect.

No difference was observed in the lesion stability index, and although we observed a slight increase in the amount of macrophages as percentage of the total plaque area, the amount of NLRP3 expression was very low and did not differ between any of the groups, indicating that the pro-inflammatory macrophage activity was not affected (26). In line with this, the percentage of pro-inflammatory Ly-6C<sup>High</sup> monocytes (35) was decreased and the percentage of non-inflammatory Ly-6C<sup>Low+Intermediate</sup> monocytes, which actively patrol the luminal site of the endothelium where they remove debris and damaged cells and are associated with reparative processes (35), was increased in OSM treated mice. The decrease in Ly-6C<sup>High</sup> monocytes plausibly contributes to the reduced amount of macrophages and the attenuated atherosclerosis development.



Although our findings are counter-intuitive with several previously described pro-inflammatory characteristics of OSM (9,36), they are in line with studies addressing the anti-inflammatory properties of OSM. It has been shown that OSM administration suppresses TNF $\alpha$  (37) and IL-1 $\beta$  release in vitro (38), whereas TNF $\alpha$ , IL-1 $\beta$  and IFN- $\gamma$  expression is increased in adipose tissue of OSMR knockout mice (39). Both cytokines are involved in atherosclerosis progression in mice as TNF $\alpha$  promotes atherosclerosis (40) and IL-1 $\beta$  knockout mice have smaller and less severe atherosclerotic lesions (41). In humans, anti-inflammatory treatments targeting TNF $\alpha$  or IL-1 $\beta$  are associated with decreased risk of myocardial infarction and overall cardiovascular events (42,43). Collectively, these and our data indicate that OSM has anti-inflammatory effects as well which may contribute to its anti-atherogenic properties. Moreover, OSM has been reported to induce endothelial proliferation (12,44) and to increase expression of adhesion molecules that bind endothelial progenitor cells (45,46), suggesting that OSM stimulates replacement of leaky, dysfunctional endothelial cells by new and healthy endothelial cells (47) and may therefore attenuate atherogenesis in the initial stages of the disease. This contention is in line with our finding that mice treated with OSM for only 5.5 weeks had a similar lesion size and severity as mice receiving OSM during a 16 week period and suggests that the observed anti-atherogenic effects of OSM have taken place during the initial stages of atherosclerosis development. Furthermore, although the observed increase in SMCs observed in this study was not significant, others have reported that OSM significantly enhances SMC proliferation in vitro (13), which is a contributor to a stable plaque phenotype (48). To conclude, OSM may contribute to attenuation of plaque development and improvement of plaque severity by: (I) its anti-inflammatory properties, (II) regenerating the endothelial barrier, (III) induction of SMC proliferation, and (IV) reducing the pro-inflammatory monocyte phenotype and promoting a more regenerative phenotype (48).

The anti-atherogenic effect of OSM in APOE\*3-Leiden.CETP mice is consistent with the increased post incident CHD survival probability in humans with higher OSM levels in the AGES-Reykjavik study. Similarly, OSM treatment increased survival in a mouse injury model of acute myocardial infarction (49), emphasizing the regenerative properties of this cytokine (44,50).

As OSM has been suggested to have a progressive effect in chronic inflammatory diseases such as, rheumatoid arthritis (RA) (51) and inflammatory bowel disease (36,52), it has been proposed as a possible pharmaceutical target to suppress inflammation in these diseases (36,51,52) and the effect of anti-OSM treatment in RA has already been investigated in a phase 2 clinical trial (51). However, considering the anti-atherogenic effects and positive effect of OSM on survival in the present study, we strongly recommend that cardiovascular disease markers and survival are carefully monitored when testing an OSM inhibiting approach. In addition, since this study shows that OSM has beneficial immune modulating effects, the role of OSM in inflammatory diseases possibly needs to be reconsidered.

Taken together, our study provides more insight into the role of OSM in atherosclerosis development. APOE\*3-Leiden.CETP mice treated with OSM had smaller and less severe plaques associated with a decrease in pro-inflammatory Ly-6C<sup>High</sup> monocytes. In line with the favorable effect in mice, we found an increased survival probability in humans that have high OSM levels, suggesting an atheroprotective effect for OSM.

### **Acknowledgements**

The authors thank Anouska Borgman (Quorics), Eveline Gart (TNO), Christa de Ruiten (TNO) and Joline Attema (TNO), for their excellent technical assistance and contribution to the data collection.

### **Disclosures**

Nothing to disclose.

### **Funding**

This work was supported by the European Union Seventh Framework Programme (FP7/2007-2013) [grant number 602936] (CaTarDis project). The funders had no role in study design, data collection and analysis, decision to publish, or preparation of the manuscript. Quorics B.V provided support in the form of salaries for authors DVK and DT, and Molecular Profiling Consulting provided salary for MDSG but did not have any additional role in the study design, data collection and analysis, decision to publish, or preparation of the manuscript.

## References

- Ramji DP, Davies TS. Cytokines in atherosclerosis: Key players in all stages of disease and promising therapeutic targets. *Cytokine Growth Factor Rev.* 2015 Dec;26(6):673–85.
- McLaren JE, Michael DR, Ashlin TG, et al. Cytokines, macrophage lipid metabolism and foam cells: implications for cardiovascular disease therapy. *Prog Lipid Res.* 2011 Oct;50(4):331–47.
- Schnittker D, Kwofie K, Ashkar A, et al. Oncostatin M and TLR-4 ligand synergize to induce MCP-1, IL-6, and VEGF in human aortic adventitial fibroblasts and smooth muscle cells. *Mediators Inflamm.* 2013;2013:317503.
- Kakutani Y, Shioi A, Shoji T, et al. Oncostatin M Promotes Osteoblastic Differentiation of Human Vascular Smooth Muscle Cells Through JAK3-STAT3 Pathway. *J Cell Biochem.* 2015 Jul;116(7):1325–33.
- Shioi A, Katagi M, Okuno Y, et al. Induction of bone-type alkaline phosphatase in human vascular smooth muscle cells: roles of tumor necrosis factor- $\alpha$  and oncostatin M derived from macrophages. *Circ Res.* 2002 Jul;91(1):9–16.
- Hurst SM, McLoughlin RM, Monslow J, et al. Secretion of oncostatin M by infiltrating neutrophils: regulation of IL-6 and chemokine expression in human mesothelial cells. *J Immunol.* 2002 Nov;169(9):5244–51.
- Thoma B, Bird TA, Friend DJ, et al. Oncostatin M and leukemia inhibitory factor trigger overlapping and different signals through partially shared receptor complexes. *J Biol Chem.* 1994 Feb;269(8):6215–22.
- Brown TJ, Rowe JM, Liu JW, et al. Regulation of IL-6 expression by oncostatin M. *J Immunol.* 1991 Oct;147(7):2175–80.
- Modur V, Feldhaus MJ, Weyrich AS, et al. Oncostatin M is a proinflammatory mediator. In vivo effects correlate with endothelial cell expression of inflammatory cytokines and adhesion molecules. *J Clin Invest.* 1997 Jul;100(1):158–68.
- van Keulen D, Pouwer MG, Pasterkamp G, et al. Inflammatory cytokine oncostatin M induces endothelial activation in macro- and microvascular endothelial cells and in APOE\*3Leiden.CETP mice. *PLoS One.* 2018;13(10):e0204911.
- Takata F, Sumi N, Nishioku T, et al. Oncostatin M induces functional and structural impairment of blood-brain barriers comprised of rat brain capillary endothelial cells. *Neurosci Lett.* 2008 Aug;441(2):163–6.
- Vasse M, Pourtau J, Trochon V, et al. Oncostatin M induces angiogenesis in vitro and in vivo. *Arterioscler Thromb Vasc Biol.* 1999 Aug;19(8):1835–42.
- Albasanz-Puig A, Murray J, Preusch M, et al. Oncostatin M is expressed in atherosclerotic lesions: a role for Oncostatin M in the pathogenesis of atherosclerosis. *Atherosclerosis.* 2011 Jun;216(2):292–8.
- Zhang X, Li J, Qin J-J, et al. Oncostatin M receptor beta deficiency attenuates atherogenesis by inhibiting JAK2/STAT3 signaling in macrophages. *J Lipid Res.* 2017 May;58(5):895–906.
- Dewey FE, Gusarova V, Dunbar RL, et al. Genetic and Pharmacologic Inactivation of ANGPTL3 and Cardiovascular Disease. *N Engl J Med.* 2017 Jul;377(3):211–21.
- Perisic L, Aldi S, Sun Y, et al. Gene expression signatures, pathways and networks in carotid atherosclerosis. *J Intern Med.* 2016 Mar;279(3):293–308.
- van Dijk RA, Virmani R, von der Thusen JH, et al. The natural history of aortic atherosclerosis: a systematic histopathological evaluation of the peri-renal region. *Atherosclerosis.* 2010 May;210(1):100–6.
- Aldi S, Matic LP, Hamm G, et al. Integrated Human Evaluation of the Lysophosphatidic Acid Pathway as a Novel Therapeutic Target in Atherosclerosis. *Mol Ther Methods Clin Dev.* 2018 Sep;10:17–28.
- Anderson CM, Zhang B, Miller M, et al. Fully Automated RNAscope In Situ Hybridization Assays for Formalin-Fixed Paraffin-Embedded Cells and Tissues. *J Cell Biochem.* 2016 Oct;117(10):2201–8.
- Harris TB, Launer LJ, Eiriksdottir G, et al. Age, Gene/Environment Susceptibility-Reykjavik Study: multidisciplinary applied phenomics. *Am J Epidemiol.* 2007 May;165(9):1076–87.
- Emilsson V, Ilkov M, Lamb JR, et al. Co-regulatory networks of human serum proteins link genetics to disease. *Science.* 2018 Aug;361(6404):769–73.
- Kuhnast S, van der Hoorn JWA, Pieterman EJ, et al. Alirocumab inhibits atherosclerosis, improves the plaque morphology, and enhances the effects of a statin. *J Lipid Res.* 2014 Oct;55(10):2103–12.
- Kuhnast S, van der Hoorn JWA, van den Hoek AM, et al. Aliskiren inhibits atherosclerosis development and improves plaque stability in APOE\*3Leiden.CETP transgenic mice with or without treatment with atorvastatin. *J Hypertens.* 2012 Jan;30(1):107–16.

24. Stary HC, Chandler AB, Dinsmore RE, et al. A definition of advanced types of atherosclerotic lesions and a histological classification of atherosclerosis. A report from the Committee on Vascular Lesions of the Council on Arteriosclerosis, American Heart Association. *Circulation*. 1995 Sep;92(5):1355–74.
25. Landlinger C, Pouwer MG, Juno C, et al. The AT04A vaccine against proprotein convertase subtilisin/kexin type 9 reduces total cholesterol, vascular inflammation, and atherosclerosis in APOE\*3Leiden.CETP mice. *Eur Heart J*. 2017 Aug;38(32):2499–507.
26. Awad F, Assrawi E, Jumeau C, et al. Impact of human monocyte and macrophage polarization on NLR expression and NLRP3 inflammasome activation. *PLoS One*. 2017;12(4):e0175336.
27. Hanna RN, Shaked I, Hubbeling HG, et al. NR4A1 (Nur77) deletion polarizes macrophages toward an inflammatory phenotype and increases atherosclerosis. *Circ Res*. 2012 Feb;110(3):416–27.
28. Therneau TM, Crowson CS, Atkinson EJ. No Adjusted Survival Curves [Internet]. 2015. Available from: <https://cran.r-project.org/web/packages/survival/vignettes/adjcurve.pdf>
29. Demyanets S, Kaun C, Rychli K, et al. The inflammatory cytokine oncostatin M induces PAI-1 in human vascular smooth muscle cells in vitro via PI 3-kinase and ERK1/2-dependent pathways. *Am J Physiol Heart Circ Physiol*. 2007 Sep;293(3):H1962-8.
30. Guihard P, Boutet M-A, Brounais-Le Royer B, et al. Oncostatin m, an inflammatory cytokine produced by macrophages, supports intramembranous bone healing in a mouse model of tibia injury. *Am J Pathol*. 2015 Mar;185(3):765–75.
31. Chistiakov DA, Orekhov AN, Bobryshev Y V. Vascular smooth muscle cell in atherosclerosis. *Acta Physiol (Oxf)*. 2015 May;214(1):33–50.
32. Seljeflot I, Tonstad S, Hjermann I, et al. Reduced expression of endothelial cell markers after 1 year treatment with simvastatin and atorvastatin in patients with coronary heart disease. *Atherosclerosis*. 2002 May;162(1):179–85.
33. Libby P. Inflammation in atherosclerosis. *Arterioscler Thromb Vasc Biol*. 2012 Sep;32(9):2045–51.
34. Zhang Q, Putheti P, Zhou Q, et al. Structures and biological functions of IL-31 and IL-31 receptors. *Cytokine Growth Factor Rev*. 2008;19(5–6):347–56.
35. Thomas G, Tacke R, Hedrick CC, et al. Nonclassical patrolling monocyte function in the vasculature. *Arterioscler Thromb Vasc Biol*. 2015 Jun;35(6):1306–16.
36. West NR, Hegazy AN, Owens BMJ, et al. Oncostatin M drives intestinal inflammation and predicts response to tumor necrosis factor-neutralizing therapy in patients with inflammatory bowel disease. *Nat Med*. 2017 May;23(5):579–89.
37. Wahl AF, Wallace PM. Oncostatin M in the anti-inflammatory response. *Ann Rheum Dis*. 2001 Nov;60 Suppl 3:iii75–80.
38. Dumas A, Lagarde S, Laflamme C, et al. Oncostatin M decreases interleukin-1 beta secretion by human synovial fibroblasts and attenuates an acute inflammatory reaction in vivo. *J Cell Mol Med*. 2012 Jun;16(6):1274–85.
39. Komori T, Morikawa Y. Oncostatin M in the development of metabolic syndrome and its potential as a novel therapeutic target. *Anat Sci Int*. 2018 Mar;93(2):169–76.
40. Boesten LSM, Zadelaar ASM, van Nieuwkoop A, et al. Tumor necrosis factor-alpha promotes atherosclerotic lesion progression in APOE\*3-Leiden transgenic mice. *Cardiovasc Res*. 2005 Apr;66(1):179–85.
41. Kirii H, Niwa T, Yamada Y, et al. Lack of interleukin-1beta decreases the severity of atherosclerosis in ApoE-deficient mice. *Arterioscler Thromb Vasc Biol*. 2003 Apr;23(4):656–60.
42. Low ASL, Symmons DPM, Lunt M, et al. Relationship between exposure to tumour necrosis factor inhibitor therapy and incidence and severity of myocardial infarction in patients with rheumatoid arthritis. *Ann Rheum Dis*. 2017 Apr;76(4):654–60.
43. Ridker PM, Everett BM, Thuren T, et al. Antiinflammatory Therapy with Canakinumab for Atherosclerotic Disease. *N Engl J Med*. 2017 Sep;377(12):1119–31.
44. Zhang X, Zhu D, Wei L, et al. OSM Enhances Angiogenesis and Improves Cardiac Function after Myocardial Infarction. *Biomed Res Int*. 2015;2015:317905.
45. Zampetaki A, Kirton JP, Xu Q. Vascular repair by endothelial progenitor cells. *Cardiovasc Res*. 2008 Jun;78(3):413–21.
46. Modur V, Li Y, Zimmerman GA, et al. Retrograde inflammatory signaling from neutrophils to endothelial cells by soluble interleukin-6 receptor alpha. *J Clin Invest*. 1997 Dec;100(11):2752–6.
47. Du F, Zhou J, Gong R, et al. Endothelial progenitor cells in atherosclerosis. *Front Biosci (Landmark Ed)*. 2012 Jun;17:2327–49.

48. Finn AV, Nakano M, Narula J, et al. Concept of vulnerable/unstable plaque. *Arterioscler Thromb Vasc Biol.* 2010 Jul;30(7):1282–92.
49. Kubin T, Poling J, Kostin S, et al. Oncostatin M is a major mediator of cardiomyocyte dedifferentiation and remodeling. *Cell Stem Cell.* 2011 Nov;9(5):420–32.
50. Nakamura K, Nonaka H, Saito H, et al. Hepatocyte proliferation and tissue remodeling is impaired after liver injury in oncostatin M receptor knockout mice. *Hepatology.* 2004 Mar;39(3):635–44.
51. Choy EH, Bendit M, McAleer D, et al. Safety, tolerability, pharmacokinetics and pharmacodynamics of an anti-oncostatin M monoclonal antibody in rheumatoid arthritis: results from phase II randomized, placebo-controlled trials. *Arthritis Res Ther.* 2013 Sep;15(5):R132.
52. Kim WM, Kaser A, Blumberg RS. A role for oncostatin M in inflammatory bowel disease. *Nat Med.* 2017 May;23(5):535–6.

